Journal of Mathematical Modeling
Vol. 13, No. 1, 2025, pp. 139–152. Research Article

JMM

A novel fractional Bernoulli-Picard iteration method to solve fractional differential equations

Fatemeh Zakipour, Abbas Saadatmandi*

Department of Applied Mathematics, Faculty of Mathematical Sciences, University of Kashan, Kashan 87317-53153, Iran
Email(s): f.zakipour70@gmail.com, saadatmandi@kashanu.ac.ir

Abstract. This paper introduces a new computational method for solving linear and non-linear fractional differential equations (FDEs). Our method essentially consists of the combination of orthonormal Bernoulli polynomials and the fractional form of the Picard iteration method. We name this method the fractional Bernoulli-Picard iteration method (FBPIM). Unlike the spectral method, the proposed method does not require solving a set of algebraic equations. We also discuss the convergence of the method. Moreover, some numerical examples are included and compared with previously published results to assess both the accuracy and suitability of the developed technique.

Keywords: Caputo derivative, Picard iteration method, orthonormal Bernoulli polynomials, fractional differential equations, numerical solution.
AMS Subject Classification 2010: 26A33, 33C47.

1 Introduction

FDEs have gained significant attention in recent years due to their ability to describe numerous real-world phenomena in various fields, including physics, engineering, biology, optimal control, and finance (see e.g., [2,3,8,14] and references therein). Unlike ordinary differential equations, FDEs involve derivatives of non-integer order, providing the ability to capture long-range dependencies and memory effects. Solving FDEs presents a challenge as traditional analytical methods are often inadequate for this task. So, over the past few decades, extensive research has been conducted on numerical approximation methods for solving FDEs. For example, we can refer to operational matrix method [12, 20, 21], collocation method [11, 19], finite difference method [1] and other methods [10, 15].

This article focuses on combining two powerful methods for solving FDEs: orthonormal Bernoulli

*Corresponding author
Received: 01 September 2024/ Revised: 24 September 2024/ Accepted: 03 October 2024
DOI: 10.22124/jmm.2024.28329.2497

polynomials (OBPs) approximation method and Picard iteration method. In recent years, various numerical methods based on the Bernoulli polynomials have been developed. For example, in 2014, Tohidi and his colleagues applied these polynomials to solve fractional integro-differential equations [27]. Nemati [19] used the Bernoulli polynomial approximation method to obtain numerical solutions for FDEs. In [13, 23], these polynomials are used for solving Fredholm-Volterra integro-differential equations of fractional order. Most recently, Rahimkhani et al. proposed a technique based on the least square support vector regression and Bernoulli wavelets for solving a system of FDEs [22]. Moreover, in [17], some advantages of employing Bernoulli polynomials instead of Legendre polynomials to approximate a function are additionally mentioned. Although Bernoulli polynomials have very interesting properties, they do not have orthogonality property. This property is particularly useful for many numerical methods. Fortunately, an explicit representation of OBPs is given in [18].

On the other hand, the Picard method, also known as Picard iteration or successive approximation method, constructs an infinite sequence of approximations to solve an equation. The core idea of the Picard method is to reformulate differential equations into integral equations. Solving an integral equation iteratively yields a series of approximations that, under certain conditions (see e.g., [7]), converge to the solution of the original differential equation. Note that it is not appropriate to use Picard's method directly as a numerical method, since computing integrals using Picard's method can be very difficult for nonlinear problems. Chebyshev-Picard iteration method was developed to solve this problem and is often used to solve ordinary differential equations (see e.g., [5, 6]). Some new works in this area can also be found in [25, 26].

To date, to our knowledge, only researchers have directly solved the FDE using Picard's successive approximation method (see e.g., [4, 16, 28]). In this paper, we generalize the Picard's method for numerically solving FDEs in a way that overcomes the drawbacks of using Picard's successive approximation method directly. This goal will be achieved by combining the Picard iteration method and the OBPs approximation. This method is called FBPIM. Some advantages of FBPIM are that

(i) this method is easily implemented.

(ii) Despite several numerical techniques, in FBPIM, there is no need to solve a set of algebraic equations.

(iii) FBPIM does not require direct calculation of fractional derivatives and integrals.

The structure of this study is as follows. Section 2 reviews some preliminaries of fractional calculus and recalling some properties related to Bernoulli polynomials. In Section 3, the fundamental formulation of FBPIM is presented. The proof of convergence of FBPIM is given in Section 4, and some numerical results are presented in Section 5. The conclusions are briefly summarized in Section 6.

2 Mathematical preliminaries

2.1 Preliminaries in fractional calculus

Both the Riemann-Liouville integral and Caputo derivative provide valuable tools in various fields of science and engineering. Their usefulness lies in their ability to handle non-local or non-integer order phenomena, providing a broader understanding and analysis of complex systems.

Definition 1. *The Riemann-Liouville fractional integral with order α is defined as [8]*

$$
\begin{aligned}
&{}_0I_x^{\alpha} z(x) = \frac{1}{\Gamma(\alpha)} \int_0^x (x-\lambda)^{\alpha-1} z(\lambda) d\lambda, \quad x>0, \ \ \alpha>0, \\
&{}_0I_x^{0} z(x) = 1,
\end{aligned} \tag{1}
$$

where $\Gamma(\cdot)$ is the Gamma function.

Definition 2. *The Caputo fractional derivative of order $\alpha > 0$ is defined as*

$$
{}_0^C D_x^{\alpha} z(x) = \tfrac{1}{\Gamma(n-\alpha)} \textstyle\int_0^x (x-\lambda)^{n-\alpha-1} z^{(n)}(\lambda) d\lambda, \qquad n-1<\alpha<n, \ n\in\mathbb{N}.
$$

$$
{}_0^C D_x^{\alpha} z(x) = z^{(n)}(x), \qquad \alpha = n.
$$

The next section uses two important properties [8]

$$
{}_0I_x^{\alpha}({}_0^C D_x^{\alpha} z(x)) = z(x) - \sum_{i=0}^{\lceil \alpha \rceil - 1} z^{(i)}(0) \frac{x^i}{i!}, \qquad x>0, \tag{2}
$$

$$
{}_0I_x^{\alpha} x^{\zeta} = \frac{\Gamma(\zeta+1)}{\Gamma(\zeta+1+\alpha)} x^{\zeta+\alpha}, \quad \alpha \geq 0, \ \ \zeta > -1, \tag{3}
$$

where $\lceil \cdot \rceil$ is the ceiling function.

2.2 Preliminaries in OBPs

The well known Bernoulli polynomials $B_n(x)$ are defined on the interval $[0,1]$ as

$$
B_n(x) = \sum_{\nu=0}^{n} \binom{n}{\nu} \beta_{\nu} x^{n-\nu}, \tag{4}
$$

where the binomial coefficients are given by $\binom{n}{\nu} = \frac{n!}{\nu!(n-\nu)!}$ and $\beta_{\nu}, \nu = 0,\ldots,n$ are Bernoulli numbers [20]. As already mentioned, Bernoulli polynomials do not have the property of orthogonality. However, their orthonormal form can be determined using the Gram-Schmidt orthonormalization method. An explicit representation of OBPs on $[0,1]$ can be introduced as follows [18]

$$
\Phi_n(x) = \sqrt{2n+1} \sum_{\nu=0}^{n} (-1)^{\nu} \binom{n}{\nu} \binom{2n-\nu}{n-\nu} x^{n-\nu}, \qquad n = 0,1,2,\ldots. \tag{5}
$$

These polynomials create an orthonormal system over $[0,1]$. Therefore, the function $z(x) \in L^2([0,1])$, can be approximated as:

$$
z(x) \approx z_N(x) = \sum_{i=0}^{N} e_i \Phi_i(x) = E\Phi(x), \tag{6}
$$

where the orthonormal Bernoulli coefficient vector E and orthonormal Bernoulli basis vector $\Phi(x)$ are given by

$$
E = [e_0, e_1, \ldots, e_N], \text{ and } \ \ \Phi(x) = [\Phi_0(x), \Phi_1(x), \ldots, \Phi_N(x)]^T. \tag{7}
$$

Here, the unique coefficients $\{e_i\}_{i=0}^{N}$ can be computed as

$$e_i = \int_0^1 z(x)\Phi_i(x)dx, \quad i = 0,1,\ldots,N.$$

Employing the Legendre-Gauss quadrature formula [21], e_i can be approximated as follows

$$e_i \approx \frac{1}{2}\sum_{j=0}^{m} z(\theta_j)\Phi_i(\theta_j)w_j, \qquad i = 0,1,\ldots,N, \tag{8}$$

where

$$\theta_j = \frac{1+t_j}{2}, \quad w_j = \frac{2}{(1-t_j^2)(P'_{m+1}(t_j))^2}, \qquad j = 0,1,\ldots,m. \tag{9}$$

Here, $P_{m+1}(t), t \in [-1,1]$ is the Legendre polynomial of order $m+1$, and $\{t_j\}_{j=0}^{m}$ are roots of $P_{m+1}(t)$. Now, using the Taylor basis functions, the Bernoulli basis vector $\Phi(x)$ given in (7), can be expressed as

$$\Phi(x) = \mathbf{B}X(x), \tag{10}$$

where $X(x) = [1,x,x^2,\ldots,x^N]^T$ is the Taylor basis vector and $\mathbf{B}$ is the change-of-basis matrix. The entries of matrix $\mathbf{B}$ can be computed using Eq. (5) as

$$\mathbf{B} = \begin{bmatrix} (-1)^0 \binom{0}{0}\binom{0}{0} & 0 & \cdots & 0 \\ \sqrt{3}(-1)^1 \binom{1}{1}\binom{1}{0} & \sqrt{3}(-1)^0 \binom{1}{0}\binom{2}{1} & \cdots & 0 \\ \vdots & \vdots & \ddots & \vdots \\ \sqrt{2N+1}(-1)^N \binom{N}{N}\binom{N}{0} & \sqrt{2N+1}(-1)^{N-1} \binom{N}{N-1}\binom{N+1}{1} & \cdots & \sqrt{2N+1}(-1)^0 \binom{N}{0}\binom{2N}{N} \end{bmatrix}.$$

The matrix $\mathbf{B}$ is nonsingular. Therefore, Eq. (10) can be expressed as

$$X(x) = \mathbf{B}^{-1}\Phi(x). \tag{11}$$

Applying ${}_0I_x^\alpha$ to Eq. (10), and using Eq. (3), we have

$${}_0I_x^\alpha\Phi(x) = {}_0I_x^\alpha(\mathbf{B}X(x)) = \mathbf{B}({}_0I_x^\alpha X(x)) = \mathbf{B}\mathbf{P}x^\alpha X(x), \tag{12}$$

where

$$\mathbf{P} = \begin{bmatrix} \frac{1}{\Gamma(1+\alpha)} & 0 & 0 & 0 & \cdots & 0 \\ 0 & \frac{1}{\Gamma(2+\alpha)} & 0 & 0 & \cdots & 0 \\ 0 & 0 & \frac{2}{\Gamma(3+\alpha)} & 0 & \cdots & 0 \\ \vdots & \vdots & \vdots & \vdots & & \vdots \\ 0 & 0 & 0 & 0 & \cdots & \frac{\Gamma(N+1)}{\Gamma(N+1+\alpha)} \end{bmatrix}.$$

By replacing Eq. (11) into Eq. (12), we get

$${}_0I_x^\alpha\Phi(x) = \mathbf{B}\mathbf{P}x^\alpha\mathbf{B}^{-1}\Phi(x) = x^\alpha\mathbf{K}\Phi(x), \tag{13}$$

where $\mathbf{K} = \mathbf{B}\mathbf{P}\mathbf{B}^{-1}$ is an $(N+1)\times(N+1)$ lower triangular matrix.

Finally, note that to apply OBPs on any interval $[a,b]$, we can use the following change of variable:

$$\widehat{x} = (b-a)x + a, \qquad 0 \le x \le 1.$$

3 Description of the method

In this section, we will explain the basic idea of FBPIM for solving FDEs. Let us consider the following single-term FDE

$$ {}_0^C D_x^\alpha v(x) = g(x, v(x)), \quad 0 \le x \le 1, \quad 0 < \alpha < 2, \tag{14} $$

with standard initial conditions:

$$ v(0) = v_a, \quad v'(0) = v'_a. \tag{15} $$

Here, the second initial condition holds only for $\alpha > 1$. First, use the transformation $z(x) = v(x) - v_a - v'_a x$ to convert the problem (14)-(15) into the following FDE with homogeneous initial conditions:

$$ \begin{aligned} {}_0^C D_x^\alpha z(x) &= h(x, z(x)), \quad 0 \le x \le 1, \quad 0 < \alpha < 2, \\ z(0) &= 0, \quad z'(0) = 0. \end{aligned} \tag{16} $$

Next, applying the fractional integral operator ${}_0I_x^\alpha$ to both sides of the FDE given in Eq. (16) and using Eq. (2), we get

$$ z(x) = \frac{1}{\Gamma(\alpha)} \int_0^x (x-\lambda)^{\alpha-1} h(\lambda, z(\lambda)) d\lambda. \tag{17} $$

Therefore, we can generate a sequence of Picard iterations as follows:

$$ z^i(x) = \frac{1}{\Gamma(\alpha)} \int_0^x (x-\lambda)^{\alpha-1} h(\lambda, z^{i-1}(\lambda)) d\lambda \quad i = 0, 1, \ldots, \tag{18} $$

where, $z^{i-1}(x)$ stands for the approximate solution at the $(i-1)$th step and $z^0(x)$ is an essential initial guess. Convergence of sequence $\{z^i(x)\}_{i=0}^{\infty}$ to $z(x)$ is discussed by [9, 28]. Now, we numerically implement Picard iteration based on the OBPs for Eq. (18). For this purpose, first we use Eq. (6) to approximate the function $h(\lambda, z^{i-1}(\lambda))$ by OBPs as:

$$ h(\lambda, z^{i-1}(\lambda)) \approx \sum_{r=0}^{N} h_r^{i-1} \Phi_r(\lambda) = H^{i-1} \Phi(\lambda), \tag{19} $$

where $H^{i-1} = [h_0^{i-1}, h_1^{i-1}, \ldots, h_N^{i-1}]$ is a coefficient vector. The coefficients $\{h_r^{i-1}\}_{r=0}^N$ can be calculated from Eq. (8) as:

$$ h_r^{i-1} \approx \frac{1}{2} \sum_{j=0}^{m} h(\theta_j, z^{i-1}(\theta_j)) \Phi_r(\theta_j) w_j, \quad r = 0, \ldots, N. \tag{20} $$

Rewriting Eq. (20) as a matrix form, we obtain

$$ \begin{aligned} H^{i-1} = \big[h(\theta_0, z^{i-1}(\theta_0)), h(\theta_1, z^{i-1}(\theta_1)), \ldots, h(\theta_m, z^{i-1}(\theta_m)) \big] \\ \times \begin{bmatrix} \frac{1}{2} w_0 & \cdots & 0 \\ \vdots & \ddots & \vdots \\ 0 & \cdots & \frac{1}{2} w_m \end{bmatrix} \begin{bmatrix} \Phi_0(\theta_0) & \cdots & \Phi_N(\theta_0) \\ \vdots & \ddots & \vdots \\ \Phi_0(\theta_m) & \cdots & \Phi_N(\theta_m) \end{bmatrix} = F^{i-1} \mathbf{WQ}, \end{aligned} \tag{21} $$

where

$$F^{i-1} = \left[h(\theta_0, z^{i-1}(\theta_0)), h(\theta_1, z^{i-1}(\theta_1)), \ldots, h(\theta_m, z^{i-1}(\theta_m))\right],$$
$$\mathbf{Q} = \begin{bmatrix} \Phi_0(\theta_0) & \cdots & \Phi_N(\theta_0) \\ \vdots & \ddots & \vdots \\ \Phi_0(\theta_m) & \cdots & \Phi_N(\theta_m) \end{bmatrix}, \quad \mathbf{W} = \begin{bmatrix} \frac{1}{2}w_0 & \ldots & 0 \\ \vdots & \ddots & \vdots \\ 0 & \cdots & \frac{1}{2}w_m \end{bmatrix}. \tag{22}$$

Note that matrices $\mathbf{Q}$ and $\mathbf{W}$ are independent of i, and the function h, so they only need to be calculated once at the beginning of the algorithm. The subsequent approximation is obtained by substituting Eq. (19) into Eq. (18):

$$\begin{aligned} z^i(x) &\approx \frac{1}{\Gamma(\alpha)} \int_0^x (x-\lambda)^{\alpha-1} \left(\sum_{r=0}^{N} h_r^{i-1} \Phi_r(\lambda) \right) d\lambda \\ &= \sum_{r=0}^{N} h_r^{i-1} \left(\frac{1}{\Gamma(\alpha)} \int_0^x (x-\lambda)^{\alpha-1} \Phi_r(\lambda) d\lambda \right) = \sum_{r=0}^{N} h_r^{i-1} ({}_0I_x^{\alpha} \Phi_r(x)). \end{aligned} \tag{23}$$

Now, we approximate $z^i(x)$ in the following form:

$$z^i(x) \approx x^{\alpha} \sum_{k=0}^{N} z_k^i \Phi_k(x) = x^{\alpha} Z^i \Phi(x), \tag{24}$$

where $Z^i = [z_0^i, z_1^i, \ldots, z_N^i]$ is an unknown vector. Using Eqs. (13), (19) and (24), we can rewrite Eq. (23) in the following vector-matrix form:

$$x^{\alpha} Z^i \Phi(x) = x^{\alpha} H^{i-1} \mathbf{K} \Phi(x). \tag{25}$$

Therefore,

$$Z^i = H^{i-1} \mathbf{K}, \tag{26}$$

where H^{i-1} is calculated using Eq. (21). Once the vector Z^i is found, the approximate solution $z^i(x)$ can be obtained from Eq. (24). The iterative process continues until the desired level of accuracy in the approximate solutions is achieved. For example, the process of creating sequence $\left\{z^i(x)\right\}_{i=0}^{\infty}$ can continue until:

$$\max\{|z^i(\theta_j) - z^{i-1}(\theta_j)|, j = 0, \ldots, m\} < \varepsilon, \tag{27}$$

where ε is a given tolerance. As you can see, there is no need to solve any set of algebraic equations to find $z^i(x)$. This is one of the most important advantages of FBPIM.

4 Convergence analysis

In this section, we discuss the convergence of FBPIM. It is important to note that, due to the use of a truncated series of OBPs at each stage and the accumulation of rounding errors, the actual domain of convergence of the FBPIM may differ from the convergence domain of the classical Picard iteration method. The norm used in this section is the maximum norm, i.e., $\|\cdot\| = \|\cdot\|_{\infty}$. Also, let $J = [0, 1]$,

$\mathbb{R}_+ = [0,\infty)$ and $C(J)$ be the Banach space of all real-valued continuous functions on J.

In sequel, we consider fractional order integral equation (17) under the following assumptions:

(i) h on $J \times \mathbb{R}_+$ is continuous and bounded with $M = \sup_{(x,z)\in J\times\mathbb{R}_+} |h(x,z)|$.

(ii) h satisfies the Lipschitz condition as

$$|h(t,z_1) - h(t,z_2)| \leq L|z_1 - z_2|,$$

where L is a real positive constant.

Lemma 1. *([9, Theorem 2.1]). Assume (i) and (ii) hold. If $LM < 1$, then (17) has a unique positive solution $z \in C(J)$.*

Lemma 2. *([9]). Let us assume that the conditions of Lemma 1 hold. In this case, all functions $z^i(x)$ obtained from Eq. (18) are continuous and the sequence $\{z^i(x)\}_{i=0}^{\infty}$ uniformly converges to $z(x) \in C(J)$. Here $z(x)$ is the exact solution of (17).*

Lemma 3. *Let $\Phi(x)$ be the orhonormal Bernoulli basis vector on the interval $[0,1]$. Then $\|\Phi(x)\| \leq \|\boldsymbol{B}\|$, where $\boldsymbol{B}$ is given in (10).*

Proof. Using Eq. (10), we have $\|\Phi(x)\| \leq \|\mathbf{B}\| \underbrace{\|X(x)\|}_{1} = \|\mathbf{B}\|$. □

Theorem 1. *Let us assume that the conditions of Lemma 2 hold. If $\Delta = L\|\boldsymbol{W}\|\|\boldsymbol{Q}\|\|\boldsymbol{K}\|\|\boldsymbol{B}\| < 1$, then the iterative scheme (18) for the FDE (16) using FBPIM converges.*

Proof. All functions $z^i(x)$ are continuous, and $z^i(x)$ can be expressed as the sum of consecutive differences

$$z^i(x) = z^0(x) + \sum_{k=1}^{n} (z^k(x) - z^{k-1}(x)).$$

Therefore, if the infinite series $\sum(z^k(x) - z^{k-1}(x))$ is convergent then the sequence $\{z^i(x)\}_{i=0}^{\infty}$ will converge to $z(x)$. Now, using Eqs. (26) and (21), we obtain

$$\begin{aligned} Z^k - Z^{k-1} &= H^{k-1}\mathbf{K} - H^{k-2}\mathbf{K} = (H^{k-1} - H^{k-2})\mathbf{K} \\ &= (F^{k-1} - F^{k-2})\mathbf{WQK}. \end{aligned} \tag{28}$$

Then, applying the triangle inequality and the Lipschitz condition, we get

$$\begin{aligned} \|Z^k - Z^{k-1}\| &\leq \|F^{k-1} - F^{k-2}\|||\mathbf{W}||||\mathbf{Q}||||\mathbf{K}|| \\ &= \max_{0\leq j\leq m} |h(\theta_j, z^{k-1}(\theta_j)) - h(\theta_j, z^{k-2}(\theta_j))|||\mathbf{W}||||\mathbf{Q}||\mathbf{K}|| \\ &\leq L \max_{0\leq j\leq m} |z^{k-1}(\theta_j) - z^{k-2}(\theta_j)|||\mathbf{W}||||\mathbf{Q}||\mathbf{K}|| \\ &\leq L||z^{k-1}(x) - z^{k-2}(x)||||\mathbf{W}||||\mathbf{Q}||||\mathbf{K}||. \end{aligned} \tag{29}$$

Using Eq. (24) and Lemma 3, we have

$$\|z^k(x) - z^{k-1}(x)\| \leq \|x^\alpha\|||Z^k - Z^{k-1}||||\Phi(x)|| \leq \|Z^k - Z^{k-1}||||\mathbf{B}||. \tag{30}$$

From (29) and (30), we obtain

$$\begin{aligned} ||z^k(x)-z^{k-1}(x)|| &\leq ||z^{k-1}(x)-z^{k-2}(x)||\Delta \\ &\leq ||z^{k-2}(x)-z^{k-3}(x)||\Delta^2 \\ &\vdots \\ &\leq ||z^1(x)-z^0(x)||\Delta^{k-1}. \end{aligned} \tag{31}$$

Since $\Delta < 1$, then the uniform convergence of $\sum_{k=1}^{\infty}(z^k(x)-z^{k-1}(x))$ is proved and as a result $\lim_{i\to\infty} z^i(x) = z(x)$. □

5 Illustrative examples

In this section, to verify the performance and accuracy of the FBPIM for solving FDEs, we present several examples. Our computations were performed by Maple programming on a personal computer equipped with 3.40 GHz, Core i7, and 4 GB of memory.

Example 1. Consider the following linear FDE [24]:

$$ {}_0^C D_x^{\alpha} z(x) + z(x) = 0, \qquad 0 < \alpha \leq 2, \tag{32}$$

with initial conditions

$$ z(0) = 1, \ \text{ if } \ 0 < \alpha < 1, \tag{33}$$

or

$$ z(0) = 1, \ \ z'(0) = 0, \ \text{if } \ 1 < \alpha < 2. \tag{34}$$

The analytical solution is $z(x) = \mathrm{E}_{\alpha}(-x^{\alpha})$, in which $\mathrm{E}_{\alpha}(x)$ is the Mittag-Leffler function defined by

$$ \mathrm{E}_{\alpha}(x) = \sum_{k=0}^{\infty} \frac{x^k}{\Gamma(k\alpha+1)}, \quad \alpha > 0. $$

Eq. (32) is referred to as the simple fractional relaxation equation and the simple fractional oscillation equation for $0 < \alpha < 1$ and $1 < \alpha < 2$ respectively [10]. The absolute errors obtained by utilizing the FBPIM, described in Section 3, with $N = m = 10, \varepsilon = 10^{-13}$ and for different values of α are illustrated in Table 1. Also, in Table 1, we have compared the absolute error of the FBPIM and the Legendre operational matrix method given in [24]. Indeed, the plotted numerical results for $z(x)$ are depicted in Figure 1, which displays the outcomes for $N = m = 20$, and different values of α, namely 0.5, 0.75, and 0.95. It is worth noting that when $\alpha = 1$, the analytical solution can be expressed as $z(x) = \exp(-x)$. Figure 1 illustrates that as the parameter α approaches 1, the numerical solution gradually converges towards the analytical solution $z(x) = \exp(-x)$. On the other hand, when $\alpha = 2$, the analytical solution becomes $z(x) = \cos(x)$. The numerical results for $z(x)$ with $N = m = 20$ and $\alpha = 1.5, 1.75, 1.95$ are displayed in Figure 2. Once again, it can be observed from Figure 2 that as α approaches 2, the numerical solution converges to the analytical solution $z(x) = \cos(x)$. These Figures demonstrate the corresponding solutions of the FDE approach to the solutions of integer order differential equation.

Table 1: Absolute error for different values of α, $N = m = 10$ and $\varepsilon = 10^{-13}$ for Example 1.

	$\alpha = 0.6$		$\alpha = 1.2$		$\alpha = 1.6$	
x	Method [24]	FBPIM	Method [24]	FBPIM	Method [24]	FBPIM
0.1	6.7×10^{-3}	9.4×10^{-5}	1.3×10^{-3}	3.5×10^{-7}	3.0×10^{-4}	1.9×10^{-8}
0.3	2.0×10^{-5}	2.1×10^{-6}	2.8×10^{-3}	5.1×10^{-7}	1.3×10^{-4}	1.1×10^{-7}
0.5	5.2×10^{-3}	4.8×10^{-6}	4.5×10^{-3}	1.0×10^{-6}	3.1×10^{-4}	2.1×10^{-7}
0.7	4.4×10^{-3}	3.8×10^{-5}	3.6×10^{-3}	1.0×10^{-6}	3.0×10^{-4}	2.1×10^{-7}
0.9	4.6×10^{-3}	2.8×10^{-5}	1.8×10^{-3}	7.2×10^{-7}	6.2×10^{-7}	2.0×10^{-7}

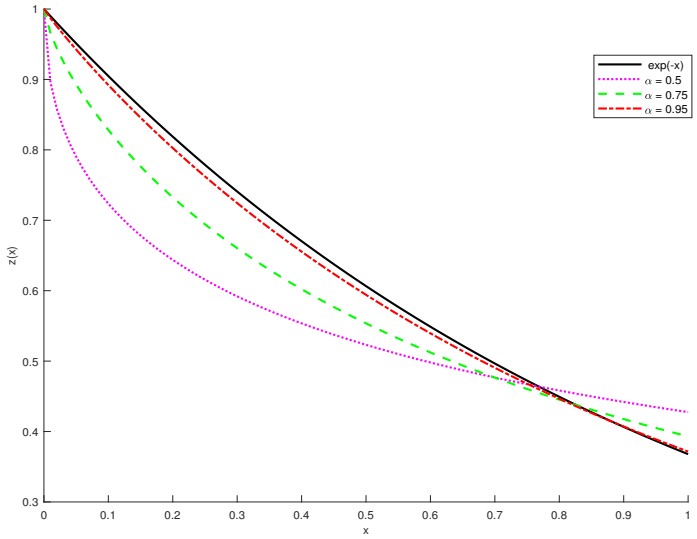

Figure 1: Numerical solutions for $\alpha = 0.5, 0.75, 0.95$, and with $N = m = 20$ and $\varepsilon = 10^{-25}$, for Example 1.

Example 2. Consider the following non-linear FDE [8, 24]

$$
\begin{aligned}
{}_0^C D_x^\alpha z(x) = & \frac{40320}{\Gamma(9-\alpha)} x^{8-\alpha} - 3\frac{\Gamma(5+\alpha/2)}{\Gamma(5-\alpha/2)} x^{4-\alpha/2} + \frac{9}{4}\Gamma(\alpha+1) \\
& + \left(\frac{3}{2}x^{\alpha/2} - x^4\right)^3 - z(x)^{3/2},
\end{aligned} \tag{35}
$$

with initial conditions

$$z(0) = 0, \ \text{ if } \ 0 < \alpha < 1, \tag{36}$$

or

$$z(0) = 0, \ \ z'(0) = 0, \ \text{if } \ 1 < \alpha < 2. \tag{37}$$

The analytical solution is given by:

$$z(x) = x^8 - 3x^{4+\alpha/2} + \frac{9}{4}x^\alpha. \tag{38}$$

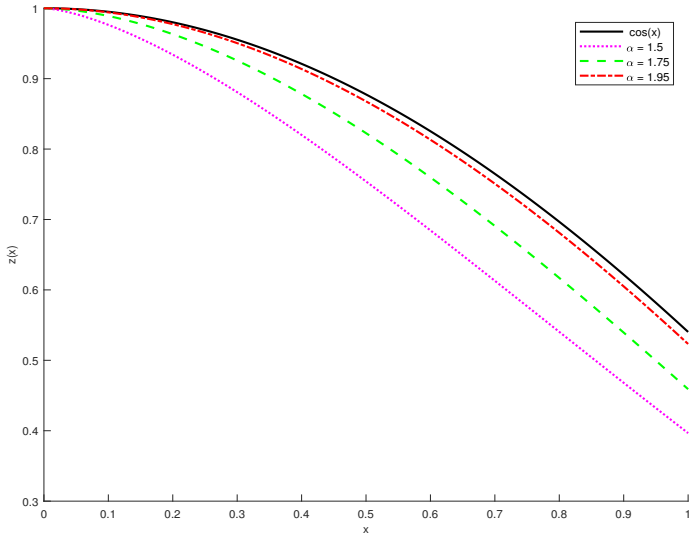

Figure 2: Numerical solutions for $\alpha = 1.5, 1.75, 1.95$, $N = m = 20$ and $\varepsilon = 10^{-25}$ for Example 1.

Table 2: Absolute error for different values of α, $N = m = 10$ and $\varepsilon = 10^{-10}$ for Example 2.

	$\alpha = 0.4$		$\alpha = 0.8$		$\alpha = 1.4$	
x	Method [24]	FBPIM	Method [24]	FBPIM	Method [24]	FBPIM
0.1	6.3×10^{-2}	9.4×10^{-8}	2.9×10^{-3}	7.0×10^{-9}	2.0×10^{-4}	5.8×10^{-8}
0.3	6.0×10^{-2}	2.5×10^{-8}	2.1×10^{-3}	9.1×10^{-8}	1.6×10^{-3}	5.2×10^{-8}
0.5	2.4×10^{-2}	5.3×10^{-8}	2.3×10^{-3}	1.9×10^{-8}	7.6×10^{-3}	4.7×10^{-8}
0.7	1.2×10^{-1}	4.6×10^{-8}	2.5×10^{-3}	6.9×10^{-8}	4.9×10^{-3}	3.1×10^{-8}
0.9	3.0×10^{-1}	4.3×10^{-8}	2.1×10^{-3}	2.9×10^{-8}	3.3×10^{-2}	7.3×10^{-9}

The Table 2, presents the absolute errors acquired through the utilization of the FBPIM, as explained in Section 3, with $N = m = 10$, $\varepsilon = 10^{-10}$, and various values of α. Additionally, the absolute error of the FBPIM is compared to the Legendre operational matrix method provided in [24] within the same Table 2. This table illustrates that our methodology yields a numerical solution that closely approximates the exact solution in comparison to the technique proposed in [24]. Also, Figures 3 and 4 illustrate the graphical representation of the absolute error functions for $\alpha = 0.7, 1.5$, and different values of $N = m$.

Example 3. Consider the following fractional Riccati differential equation [29]:

$$ {}_0^C D_x^\alpha z(x) = -z^2(x) + 2z(x) + 1, \qquad 0 < \alpha \leq 1, \tag{39} $$

with initial condition $z(0) = 0$. The analytical solution for $\alpha = 1$ is given by:

$$ z(x) = 1 + \sqrt{2} \tanh\left(\sqrt{2}x + \ln(\sqrt{2} - 1)\right). $$

The graphical depiction of the absolute error functions for $\alpha = 1$ and varying values of $N = m$ are illustrated in Figure 5. This figure demonstrates a rapid decrease in absolute errors as both N and m

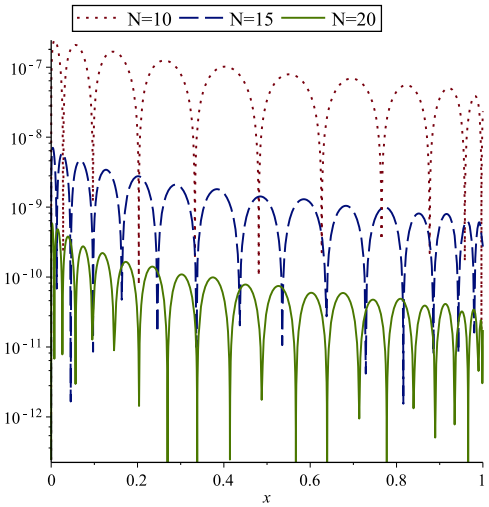

Figure 3: Graph of absolute error functions with $\alpha = 0.7$, $\varepsilon = 10^{-10}$ and for various values of $N = m$, for Example 2.

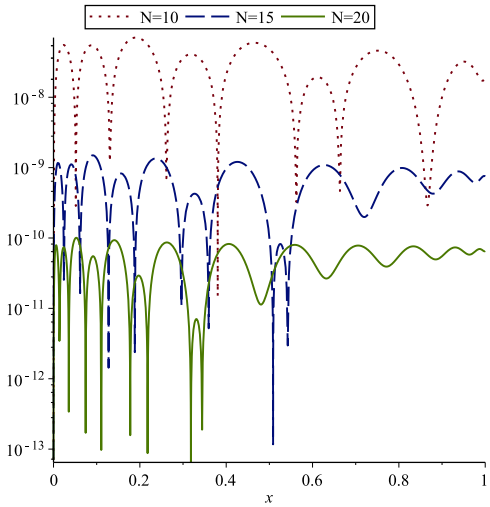

Figure 4: Graph of absolute error functions with $\alpha = 1.5$, $\varepsilon = 10^{-10}$ and for various values of $N = m$, for Example 2.

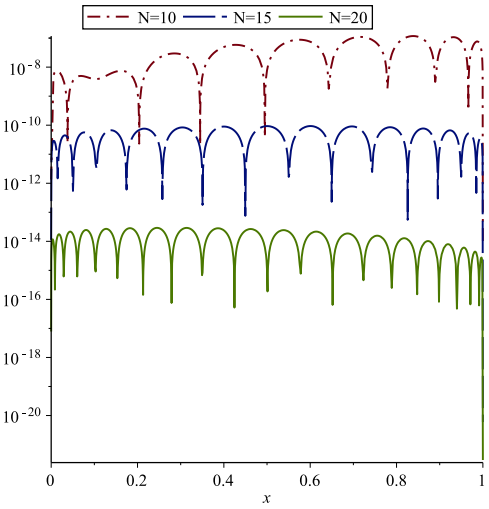

Figure 5: Graph of absolute error functions with $\alpha = 1$, $\varepsilon = 10^{-15}$ and for various values of $N = m$, for Example 3.

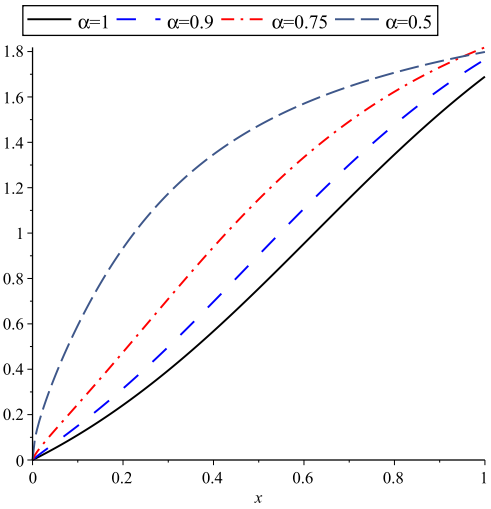

Figure 6: Numerical solutions with $\alpha = 0.5, 0.75, 0.9, 1$, $N = m = 10$ and $\varepsilon = 10^{-10}$, for Example 3.

are increased. Also, the results for different values of α are shown in Figure 6. Figure 6 shows the convergence of the numerical solution to the analytical solution as α approaches 1.

Furthermore, the maximum absolute error (denoted by $L_\infty-$error) and CPU time (in seconds) of FBPIM for all three examples and various values of $N = m$ are presented in Table 3. By increasing the value of N, it can be clearly observed from Table 3 that the $L_\infty-$errors decrease.

Table 3: Maximum absolute error and CPU time for different values of $N = m$ and $\varepsilon = 10^{-15}$.

	Example 1	($\alpha = 0.8$)	Example 2	($\alpha = 0.8$)	Example 3	($\alpha = 1$)
N	$L_\infty-$error	CPU time	$L_\infty-$error	CPU time	$L_\infty-$error	CPU time
7	2.0×10^{-4}	1.467	7.3×10^{-5}	0.593	1.8×10^{-5}	0.812
10	6.2×10^{-5}	1.778	2.2×10^{-7}	0.718	1.2×10^{-7}	1.046
15	1.8×10^{-5}	3.120	5.9×10^{-9}	0.936	9.3×10^{-11}	1.841
20	7.2×10^{-6}	7.707	4.5×10^{-10}	1.607	2.9×10^{-14}	3.807

6 Conclusion

In this paper, we have developed the FBPIM for solving FDEs. Our method distinguishes itself from other methods such as Galerkin and collocation methods by avoiding the need to solve a system of algebraic equations in order to determine the solution. The FBPIM has been effectively utilized for solving both linear and non-linear FDEs. In our computational investigations, we have presented the outcomes derived by utilizing the FBPIM on different FDEs. In general, the FBPIM presents a significant method for computationally resolving FDEs and holds promise for broader implementation in the discipline.

References

[1] M. Abbaszadeh, A. Bagheri Salec, A. Al-Khafaji, S. Kamel, *The effect of fractional-order derivative for pattern formation of Brusselator reaction-diffusion model occurring in chemical reactions*, Iranian J. Math. Chem. **14** (2023) 243–269.

[2] W.M. Abd-Elhameed, Y.H. Youssri, A.G. Atta, *Tau algorithm for fractional delay differential equations utilizing seventh-kind Chebyshev polynomials*, J. Math. Model. **12** (2024) 277–299.

[3] R. Akbari, L. Navaei, *Fractional dynamics of infectious disease transmission with optimal control*, Math. Interdisc. Res. **9** (2024) 199–213.

[4] R. Almeida, A.B. Malinowska, M.T.T. Monteiro, *Fractional differential equations with a Caputo derivative with respect to a Kernel function and their applications*, Math. Methods Appl. Sci. **41** (2018) 336–352.

[5] X. Bai, J.L. Junkins, *Modified Chebyshev-Picard iteration methods for solution of boundary value problems*, J. Astronaut. Sci. **58** (2011) 615–642.

[6] X. Bai, J.L. Junkins, *Modified Chebyshev-Picard iteration methods for solution of initial value problems*, J. Astronaut. Sci. **59** (2012) 327–351.

[7] W.J. Coles, T.L. Sherman, *Convergence of successive approximations for nonlinear two-point boundary value problems*, SIAM J. Appl. Math. **15** (1967) 426–433.

[8] K. Diethelm, *The Analysis of Fractional Differential Equations*, Springer-Verlag, Berlin, 2010.

[9] A.M.A. El-Sayed, H.H.G. Hashem, E.A.A. Ziada, *Picard and Adomian decomposition methods for a quadratic integral equation of fractional order*, Comput. Appl. Math. **33** (2014) 95–109.

[10] S. Esmaeili, M. Shamsi, M. Dehghan, *Numerical solution of fractional differential equations via a Volterra integral equation approach*, Open Phys. **11** (2013) 1470–1481.

[11] S. Esmaeili, M. Shamsi, Y. Luchko, *Numerical solution of fractional differential equations with a collocation method based on Müntz polynomials*, Comput. Appl. Math, **62** (2011) 918–929.

[12] E. Keshavarz, Y. Ordokhani, M. Razzaghi, *Bernoulli wavelet operational matrix of fractional order integration and its applications in solving the fractional order differential equations*, Appl. Math. Modelling, **38** (2014) 6038–6051.

[13] E. Keshavarz, Y. Ordokhani, M. Razzaghi, *Numerical solution of nonlinear mixed Fredholm-Volterra integro-differential equations of fractional order by Bernoulli wavelets*, Comput. Methods Differ. Equ. **7** (2019) 163–176.

[14] A.A. Kilbas, H.M. Srivastava, J.J. Trujillo, *Theory and Applications of Fractional Differential Equations*, Elsevier, San Diego, 2006.

[15] P. Kumar, O.P. Agrawal, *An approximate method for numerical solution of fractional differential equations*, Signal Process. **86** (2006) 2602–2610.

[16] R. Lyons, A.S. Vatsala, R.A. Chiquet, *Picard's iterative method for Caputo fractional differential equations with numerical results*, Mathematics, **5** (2017) 65.

[17] S. Mashayekhi, Y. Ordokhani, M. Razzaghi, *Hybrid functions approach for nonlinear constrained optimal control problems*, Commun. Nonlinear Sci. Numer. Simul. **17** (2012) 1831–1843.

[18] F. Mirzaee, N. Samadyar, *Explicit representation of orthonormal Bernoulli polynomials and its application for solving Volterra-Fredholm-Hammerstein integral equations*, SeMA J. **77** (2020) 81–96.

[19] S. Nemati, P.M. Lima, D.F. Torres, *Numerical solution of variable-order fractional differential equations using Bernoulli polynomials*, Fractal fract. **5** (2021) 219.

[20] M. Pourbabaee, A. Saadatmandi, *New operational matrix of Riemann-Liouville fractional derivative of orthonormal Bernoulli polynomials for the numerical solution of some distributed-order time-fractional partial differential equations*, J. Appl. Anal. Comput. **13** (2023) 3352–3373.

[21] M. Pourbabaee, A. Saadatmandi, *A new operational matrix based on Müntz-Legendre polynomials for solving distributed order fractional differential equations*, Math. Comput. Simulat. **194** (2022) 210–235.

[22] P. Rahimkhani, Y. Ordokhani, S. Sabermahani, *Bernoulli wavelet least square support vector regression: Robust numerical method for systems of fractional differential equations*, Math. Methods Appl. Sci. **46** (2023) 17641–17659.

[23] A. Saadatmandi, S. Akhlaghi, *Using hybrid of block-pulse functions and Bernoulli polynomials to solve fractional Fredholm-Volterra integro-differential equations*, Sains Malays. **49** (2020) 953–962.

[24] A. Saadatmandi, M. Dehghan, *A new operational matrix for solving fractional-order differential equations*, Comput. Math. Appl. **59** (2010) 1326–1336.

[25] M. Tafakkori-Bafghi, G.B. Loghmani, M. Heydari, *Numerical solution of two-point nonlinear boundary value problems via Legendre-Picard iteration method*, Math. Comput. Simul. **199** (2022) 133–159.

[26] M. Tafakkori-Bafghi, G.B. Loghmani, M. Heydari, X. Bai, *Jacobi-Picard iteration method for the numerical solution of nonlinear initial value problems*, Math. Methods Appl. Sci. **43** (2020) 1084–1111.

[27] E. Tohidi, M.M. Ezadkhah, S. Shateyi, *Numerical solution of nonlinear fractional Volterra integro-differential equations via Bernoulli polynomials*, Abstr. Appl. Anal. **2014** (2014) 162896.

[28] X. Yang, Y. Liu, *Picard iterative processes for initial value problems of singular fractional differential equations*, Adv. Differ. Equ. **2014** (2014) 102.

[29] Ş. Yüzbaşı, *Numerical solutions of fractional Riccati type differential equations by means of the Bernstein polynomials*, Appl. Math. Comput. **219** (2013) 6328–6343.